Check for updates

Received: 17 February 2023 | Revised: 2 May 2023 | Accepted: 25 May 2023

DOI: 10.1111/aor.14593

Artificial Organs WILEY

MAIN TEXT

Closed-loop parameter optimization for patient-specific phrenic nerve stimulation

Conor Keogh[1] | Francisco Saavedra[1,2] | Sebastian Dubo[3] | Pablo Aqueveque[2] | Paulina Ortega[3] | Britam Gomez[2] | Enrique Germany[2] | Daniela Pinto[2] | Rodrigo Osorio[2] | Francisco Pastene[2] | Adrian Poulton[1] | Jonathan Jarvis[4] | Brian Andrews[1] | James J. FitzGerald[1]

[1]Nuffield Department of Surgical Sciences, University of Oxford, Oxford, UK

[2]Department of Electrical Engineering, Universidad de Concepcion, Concepcion, Chile

[3]Department of Physiotherapy, Universidad de Concepcion, Concepcion, Chile

[4]School of Sports and Exercise Science, Liverpool John Moores University, Liverpool, UK

Correspondence
Conor Keogh, Nuffield Department of Surgical Sciences, University of Oxford, Oxford, UK.
Email: conor.keogh@nds.ox.ac.uk

Funding information
Engineering and Physical Sciences Research Council; National Institute for Health and Care Research; University of Oxford

Abstract

Background: Ventilator-induced diaphragm dysfunction occurs rapidly following the onset of mechanical ventilation and has significant clinical consequences. Phrenic nerve stimulation has shown promise in maintaining diaphragm function by inducing diaphragm contractions. Non-invasive stimulation is an attractive option as it minimizes the procedural risks associated with invasive approaches. However, this method is limited by sensitivity to electrode position and inter-individual variability in stimulation thresholds. This makes clinical application challenging due to potentially time-consuming calibration processes to achieve reliable stimulation.

Methods: We applied non-invasive electrical stimulation to the phrenic nerve in the neck in healthy volunteers. A closed-loop system recorded the respiratory flow produced by stimulation and automatically adjusted the electrode position and stimulation amplitude based on the respiratory response. By iterating over electrodes, the optimal electrode was selected. A binary search method over stimulation amplitudes was then employed to determine an individualized stimulation threshold. Pulse trains above this threshold were delivered to produce diaphragm contraction.

Results: Nine healthy volunteers were recruited. Mean threshold stimulation amplitude was 36.17 ±14.34 mA (range 19.38–59.06 mA). The threshold amplitude for reliable nerve capture was moderately correlated with BMI (Pearson's $r=0.66$, $p=0.049$). Repeating threshold measurements within subjects demonstrated low intra-subject variability of 2.15 ±1.61 mA between maximum and minimum thresholds on repeated trials. Bilateral stimulation with individually optimized parameters generated reliable diaphragm contraction, resulting in significant inhaled volumes following stimulation.

Conclusion: We demonstrate the feasibility of a system for automatic optimization of electrode position and stimulation parameters using a closed-loop system.

This is an open access article under the terms of the Creative Commons Attribution License, which permits use, distribution and reproduction in any medium, provided the original work is properly cited.
© 2023 The Authors. *Artificial Organs* published by International Center for Artificial Organ and Transplantation (ICAOT) and Wiley Periodicals LLC.

This opens the possibility of easily deployable individualized stimulation in the intensive care setting to reduce ventilator-induced diaphragm dysfunction.

KEYWORDS

closed loop, critical care, electrical stimulation, phrenic nerve, ventilator induced diaphragm dysfunction

1 | INTRODUCTION

Mechanical ventilation is a key intervention in critical care medicine. However, the resulting disuse of the diaphragm can produce significant dysfunction, including atrophy and sarcomere injury, following even very brief periods, with significant muscle dysfunction evident after even 24 h of ventilation.[1] The resulting pathological changes, termed ventilator-induced diaphragm dysfunction, alter its contractile function and result in difficulty weaning from the ventilator and poor clinical outcomes,[2] and are thought to be caused by loss of muscle activity, as particularly occurs during mandatory modes of ventilation, leading to atrophy.[3]

Stimulation of the phrenic nerve has been proposed as a promising strategy to reduce this ventilator-induced diaphragm dysfunction.[4] By activating the phrenic nerve with electrical stimulation, the diaphragm is forced to contract, "exercising" it and potentially preserving its function in a manner analogous to the application of neuromuscular electrical stimulation to avoid muscle atrophy in patients in the intensive care setting.[5] Methods such as trans-venous,[6,7] percutaneous,[8] and direct surgical[9,10] implantation of stimulation electrodes have shown some success, while other approaches such as specialized esophageal electrodes are in the early stages of development.[11] These methods are, however, limited by the need for specific technical skills for application and procedural risks due to their invasive nature.

Non-invasive methods of stimulating the phrenic nerve are attractive to improve outcomes while reducing the risks associated with intervention.[12] Frames,[13] collars,[14,15] and hand-held probes[16] have been used historically, while recent evidence has shown that surface electrodes can produce reliable diaphragm contraction without the application of pressure. With appropriate parameter selection, these methods appear to allow selective activation of the phrenic nerve without activation of off-target structures such as the vagus nerve.[12]

Non-invasive approaches are, however, limited by their sensitivity to electrode positioning and the variability in stimulation parameters between individuals. This makes translation to a clinical setting challenging due to the potentially significant time taken to perform calibration and parameter selection. The high sensitivity to electrode position makes accurate positioning vital, while the variability in optimal positioning between individuals means that application of a system that uses surface electrodes risks requiring time-consuming manual calibration of electrode position. Similarly, intra-individual variability in the stimulation amplitude required to produce protective diaphragm contractions risks requiring extensive individual parameter adjustments, or a high likelihood of either under- or over-stimulating if a single set of parameters are used for all patients, risking either insufficient or excessive activation.

Our group developed a non-invasive stimulation system suitable for maintaining contractile diaphragm activity in mechanically ventilated patients.[12] Here, we aimed to test an integrated system for real-time, closed-loop optimization of electrode location and stimulation parameters during non-invasive phrenic nerve stimulation in healthy participants with minimal off-target effects without the need for manual calibration. By measuring the respiratory flow produced following stimulation, the stimulation parameters can be automatically adjusted in order to ensure optimal diaphragm activation.

We show that this approach reliably produces stimulation with optimized parameters without the need for user input. This represents a significant step toward personalized non-invasive neuromodulation in a critical care environment for the treatment of ventilator-induced diaphragm dysfunction.

2 | METHODS

Nine healthy volunteers (six male, three female) were recruited after obtaining written informed consent. Mean participant age was 26.67 ± 2.36 years (range 23–29 years), mean height was 175.33 ± 7.10 cm (range 165–190 cm) and mean weight was 71.78 ± 11.45 kg (range 48–88 kg). The study was approved by the University of Oxford Central University Research Ethics Committee (approval reference R73898/RE001).

Participants breathed normally through a pitot tube section of an anesthetic circuit to record the flow produced. A nose clip was worn to prevent escape of air. Spirometric

15251594, 2024, 3, Downloaded from https://onlinelibrary.wiley.com/doi/10.1111/aor.14593 by Test, Wiley Online Library on [19/05/2024]. See the Terms and Conditions (https://onlinelibrary.wiley.com/terms-and-conditions) on Wiley Online Library for rules of use; OA articles are governed by the applicable Creative Commons License

measures were taken in all subjects in order to assess pulmonary function. Peak flow, forced expiratory volume in one second (FEV1), forced vital capacity (FVC) and the FEV1/FVC ratio were measured in all participants.

Linear electrode arrays were constructed and positioned unilaterally on the neck as shown in Figure 1. Electrodes were placed on the right-hand side of all participants for initial trials of threshold detection. Subsequent tests were performed using electrodes placed on the left and bilaterally in order to assess the effects of bilateral stimulation and of the laterality of stimulation. Six 1 cm ×1 cm Axelgaard electrodes were positioned with 2 mm intervals within a surrounding anode. The medial edge of the array was placed at the level of the cricoid cartilage in the midline. Electrodes had a typical impedance of 1470 ±148 Ω.

2.1 | Closed-loop control system

Electrode arrays were connected to a custom closed-loop control system for delivering stimulation and measuring the respiratory response (Figure 1C). Stimulation was applied using a current-controlled stimulator with a compliance voltage of 400 V (Digitimer DS8R). Biphasic, charge-balanced, symmetric waveforms were used throughout.

The stimulator was controlled using a custom control system based on the ARM Cortex M7 microcontroller (ST Microelectronics). The control system was configured to detect respiratory phase. Stimulation was then automatically triggered at the onset of inspiration, allowing for the delivery of stimulation to be synchronized with the respiratory cycle.

This system controlled electrode selection, stimulation parameters, and triggering of the stimulator. The respiratory response to stimulation was measured using a flow sensor (Sensirion SFM3300) in line with the respiratory circuit. These measurements were then used for automatic parameter adjustment.

2.2 | Automated electrode selection

The optimal electrode location for stimulation of the phrenic nerve was automatically determined by applying single biphasic, charge-balanced stimulation pulses

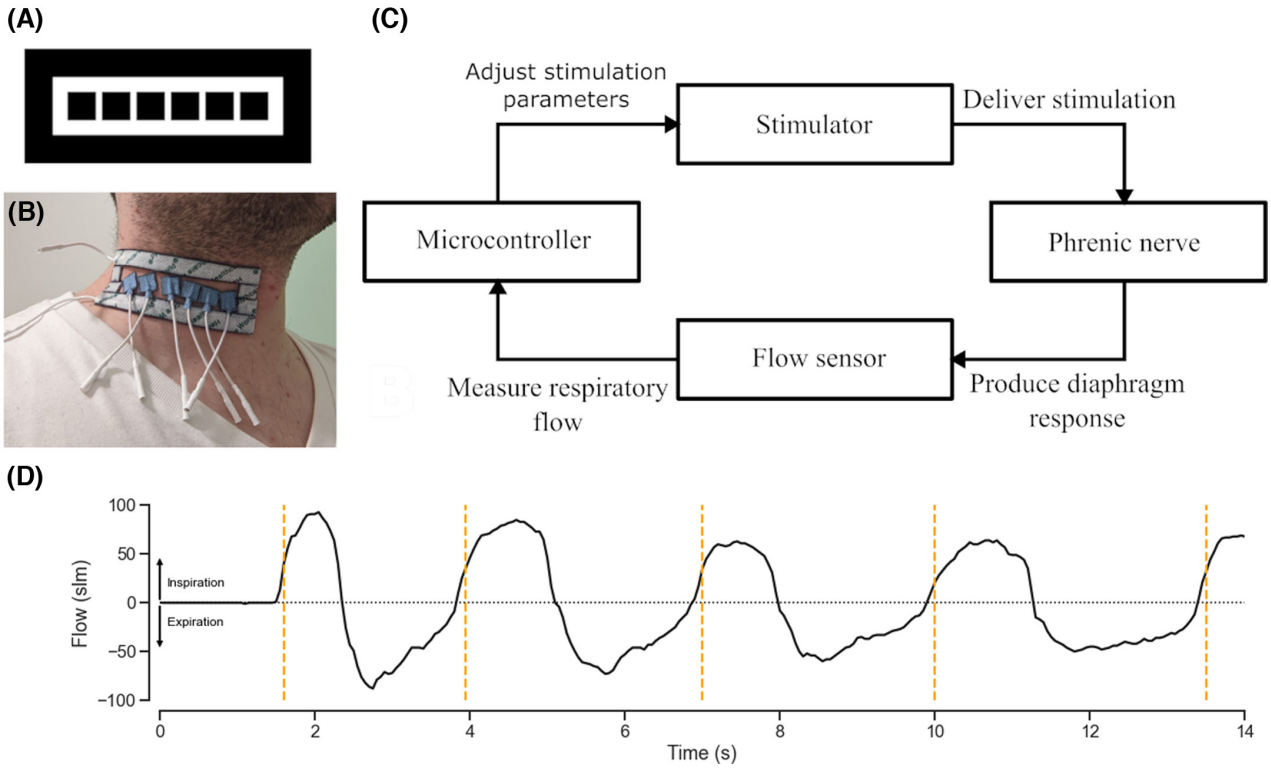

FIGURE 1 Electrode array and closed loop system schematic. (A) Schematic of electrode design. Six 1 cm ×1 cm cathodes are separated by 2 mm intervals and surrounded by an anode. (B) Photograph of electrode arrangement in situ. (C) Flowchart of system design. A stimulator delivers stimulation pulses to the phrenic nerve. The respiratory response is measured using a flow sensor. A microcontroller records the response to stimulation and adjusts the stimulation parameters. (D) Respiration-synchronized stimulation. By using the flow signal as an input, the system can detect the onset of inspiration and synchronize the delivery of stimulation with the respiratory cycle (stimulation triggers shown in orange). slm, standard liters per minute. [Color figure can be viewed at wileyonlinelibrary.com]

15251594, 2024, 3, Downloaded from https://onlinelibrary.wiley.com/doi/10.1111/aor.14593 by Test, Wiley Online Library on [19/05/2024]. See the Terms and Conditions (https://onlinelibrary.wiley.com/terms-and-conditions) on Wiley Online Library for rules of use; OA articles are governed by the applicable Creative Commons License

sequentially at each cathode and measuring the response. Based on previous studies of the strength-duration characteristics of the phrenic nerve,[12] initial determination of the optimal electrode was performed using single biphasic, charge-balanced pulses of 100 μs per phase at 50 mA as this amplitude was sufficient to produce capture in most participants in previous studies.

The respiratory response to single pulses was measured by sampling for 0.5 s at 1 kHz the flow produced following stimulation, that is, post-stimulation flow at an electrode e is given by:

$$flow(e) = [x_0, \ \dots \ , x_T]$$

where x is the sampled flow and T is the total number of samples recorded.

The response to stimulation is then quantified by calculating the area under the curve of the resulting flow signal, that is, the total volume inhaled following stimulation:

$$response(e) = \int_0^T flow(e) \cdot dt$$

The optimal electrode is then simply the electrode (e) that produces the maximum respiratory response from the set of all available electrodes (E):

$$e_{optimal} = \underset{e \in E}{\operatorname{argmax}}\, response(e)$$

The optimal electrode is automatically determined by iterating over all possible cathodes and then used for all further steps.

2.3 | Amplitude threshold optimization

The minimum amplitude required to produce a response at the optimal cathode was determined in order to provide patient-specific stimulation parameters. This overcomes the issue of inter-individual variability in thresholds.

A binary search algorithm was used to determine the stimulation threshold with a maximum amplitude of 150 mA, a minimum amplitude of 0 mA and a precision of 1 mA:

$$a_{max} = 150$$

$$a_{min} = 0$$

$$p = 1$$

This provides a high degree of resolution over a range that should reliably produce activity in all individuals while remaining within safe limits.[12] 150 mA was selected as a maximum value as this represents a level which should result in nerve capture in all participants if electrodes are positioned appropriately, and amplitudes above this are likely to produce significant discomfort.

The mean and standard deviation of the respiratory flow was measured during a 10-s period of normal breathing. A response to stimulation was then defined as a maximum flow after stimulation of greater than three standard deviations from the mean flow, that is:

$$outcome(a) = \begin{cases} 1 \text{ if } \max flow(e) > \mu_{flow} + 3\sigma_{flow} \\ 0 \text{ if } \max flow(e) < \mu_{flow} + 3\sigma_{flow} \end{cases}$$

where a is the applied amplitude at the current step of the algorithm, $flow(e)$ is the flow produced by stimulation at the specified electrode as defined above, μ_{flow} is the mean flow and σ_{flow} the standard deviation of flow over a period of normal breathing. This provides a binary measure of whether a statistically significant effect of stimulation on respiratory flow is produced for any given stimulation amplitude.

Stimulation pulses were applied at the midpoint between the minimum and maximum amplitudes at each iteration:

$$a = \frac{a_{max} + a_{min}}{2}$$

Therefore, the amplitude at any given step is determined by the current acceptable maximum and minimum stimulation amplitudes.

If a response was detected, the maximum amplitude was reduced to the current amplitude; if no response was detected, the minimum amplitude was increased to the current amplitude:

$$\begin{cases} \text{if } outcome(a) = 1 \text{: } a_{max} = a \\ \text{if } outcome(a) = 0 \text{: } a_{min} = a \end{cases}$$

The maximum and minimum acceptable amplitudes were therefore iteratively altered according to the individual response to stimulation based on whether a significant response was produced.

This process was repeated until the minimum and maximum agreed to within the specified precision, at which point the activation threshold was detected:

$$\text{if } \left(a_{max} - a_{min}\right) < p \text{: } a_{threshold} = a$$

The individualized activation threshold, $a_{threshold}$, then defines the minimum stimulation amplitude required to produce a statistically significant respiratory response in that individual.

15251594, 2024, 3, Downloaded from https://onlinelibrary.wiley.com/doi/10.1111/aor.14593 by Test, Wiley Online Library on [19/05/2024]. See the Terms and Conditions (https://onlinelibrary.wiley.com/terms-and-conditions) on Wiley Online Library for rules of use; OA articles are governed by the applicable Creative Commons License

Individualized amplitude thresholds were measured in all participants on three separate trials in order to provide measures of inter- and intra-subject variability in thresholds. Measurements were repeated in a single subject for 10 trials in order to further characterize the intra-individual variability on a larger number of trials.

2.4 | Pulse train generation

The ability of the automatically determined parameters to produce a more powerful diaphragm response was tested by delivering a 200 ms pulse train of 100 μs pulses at 50 Hz, using 125% of the individualized threshold amplitude through the optimal electrode. The respiratory response was then recorded to quantify the response to a pulse train with optimized parameters. This allowed for the response to stimulation using automatically individualized stimulation parameters to be assessed.

Initial tests of the response to pulse trains were performed with bilateral electrode arrays. Measurements were then repeated with left-sided and right-sided electrode arrays unilaterally in order to verify whether laterality has influenced the response to stimulation and whether bilateral stimulation produces a greater response than unilateral stimulation.

2.5 | Effect of burst length

While single stimulation pulses offer a rapid means of iterating over stimulation amplitudes in order to determine individualized thresholds, the actual amplitude threshold required to produce a detectable respiratory response is likely to differ between single pulses and extended bursts. The use of single pulses for individualized threshold detection therefore risks over-estimating the required stimulation amplitude.

To investigate this and to determine whether short bursts would provide better estimates of the minimum amplitude required to produce a reliable response, the process of automatically determining individualized stimulation thresholds using a binary search method was repeated for doublets (bursts of two stimulation pulses), triplets (bursts of three stimulation pulses), short bursts of five pulses and full bursts of 10 pulses, that is, equivalent to the full delivered pulse train. In all instances, stimulation was delivered at 50 Hz with a pulse width of 100 μs.

The minimum amplitude required to produce a respiratory response could then be examined as a function of the duration of the applied stimulation burst, allowing determination of the optimal burst duration for automated calibration of stimulation parameters.

3 | RESULTS

3.1 | Participants

Nine healthy volunteers were recruited (six male, three female). Demographic data and the results of spirometric testing of lung function are shown in Table 1. Participants had a mean peak flow of 540 ± 125 mL (range 301–699 mL), a mean FEV1 of 2.92 ± 1.16 L (range 1.01–4.79 L), a mean FVC of 3.56 ± 1.27 L (range 1.47–5.80), and a mean FEV1/FVC ratio of 0.80 ± 0.11 (range 0.60–0.95).

3.2 | Electrode selection

An example recording showing the ability of the system to accurately identify the onset of inspiration in order to

TABLE 1 Participant demographics and lung function tests.

Participant	Age	Height (cm)	Weight (kg)	BMI	Peak flow (L/min)	FEV1 (L)	FVC (L)	FEV1/FVC
1	29	175	75	24	654	3.25	3.93	0.83
2	29	175	70	23	646	3.25	3.93	0.83
3	25	190	88	24	550	4.35	5.80	0.75
4	28	165	48	18	301	1.36	2.29	0.60
5	29	177	85	27	699	4.79	5.08	0.94
6	28	165	65	24	473	3.17	3.75	0.84
7	23	180	70	22	637	2.60	2.74	0.95
8	26	175	65	21	411	1.01	1.47	0.68
9	23	176	80	26	489	2.49	3.03	0.82

Abbreviations: FEV1, forced expiratory volume in one second; FVC, forced vital capacity.

15251594, 2024, 3, Downloaded from https://onlinelibrary.wiley.com/doi/10.1111/aor.14593 by Test, Wiley Online Library on [19/05/2024]. See the Terms and Conditions (https://onlinelibrary.wiley.com/terms-and-conditions) on Wiley Online Library for rules of use; OA articles are governed by the applicable Creative Commons License

trigger respiration-synchronized stimulation is shown in Figure 1D.

Automatic stimulation with biphasic, charge-balanced single pulses at each cathode in an array and measurement of the respiratory response allows rapid and reliable detection of the optimal stimulating electrode. Figure 2 shows an example of the respiratory responses recorded following stimulation at each element in a linear array. There is a strong response at electrode 4, with relatively little response at any other electrodes. The optimal electrode can be reliably identified by the total volume inhaled following stimulation (i.e., the area under the curve (AUC) of the flow signal). This allows for rapid and automated detection of optimal electrode positioning for non-invasive phrenic nerve stimulation.

This approach uses a simple, easily interpretable metric to determine the optimal stimulating electrode. The use of single pulses produces reliable results and allows rapid determination of the optimal electrode. In the case of six electrodes with a response based on 0.5 s of respiratory flow, the optimal electrode for any individual can be computed in 3 s, allowing efficient and reproducible optimization of stimulation site. This overcomes existing issues with inter-individual variation in optimal electrode position, eliminates the need for manual calibration and ensures reliable activation even if there are changes in the relationship between the stimulating electrodes and underlying nerve as the optimal electrode can be rapidly re-calculated.

3.3 | Threshold detection

Binary search over stimulation amplitudes allows rapid determination of individualized stimulation thresholds using a closed-loop system. Figure 3A shows the automated adjustment of stimulation amplitude over repeated iterations while the response is measured until the system converges on the stimulation threshold. This threshold agrees with the manually measured threshold with a precision of better than 1 mA. On average, eight iterations are required to find an individualized threshold between 0 mA and 150 mA with a precision of 1 mA, providing rapid individualization of stimulation parameters.

Figure 3B shows an example of the flow produced following stimulation with a single pulse at 5 mA above the automatically determined threshold, while Figure 3C shows an example of the flow produced at 5 mA below this threshold. Stimulation above the threshold produces a strong response, while there is no response below the threshold. This confirms the accuracy of the automatically detected parameters.

It was possible to accurately determine an individualized threshold in all participants. The mean threshold across all participants was 36.17 ±14.34 mA (range 19.38–59.06 mA). The threshold required to produce reliable nerve capture in an individual was moderately correlated with body mass index (Pearson's $r = 0.66$, $p = 0.049$; Figure 4). Within individuals, there was a mean total variation in measured threshold between trials (i.e., difference

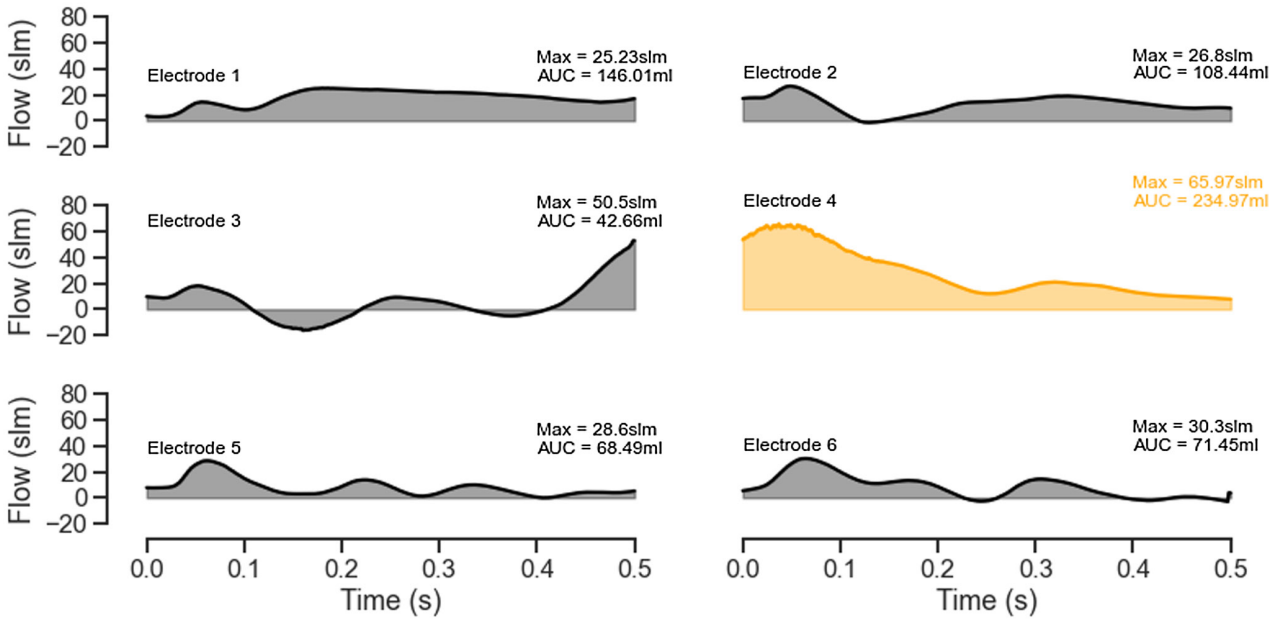

FIGURE 2 Automated electrode selection. Example flow recorded for 0.5 s following single pulses at each electrode. Respiratory response is sensitive to electrode position. Electrode 4 produced the largest response, with little response at other electrodes. Measurement of the maximum flow produced and the area under the curve (i.e., volume inhaled) allows automated detection of the optimal electrode. AUC, area under the curve; slm, standard liters per minute. [Color figure can be viewed at wileyonlinelibrary.com]

15251594, 2024, 3, Downloaded from https://onlinelibrary.wiley.com/doi/10.1111/aor.14593 by Test, Wiley Online Library on [19/05/2024]. See the Terms and Conditions (https://onlinelibrary.wiley.com/terms-and-conditions) on Wiley Online Library for rules of use; OA articles are governed by the applicable Creative Commons License

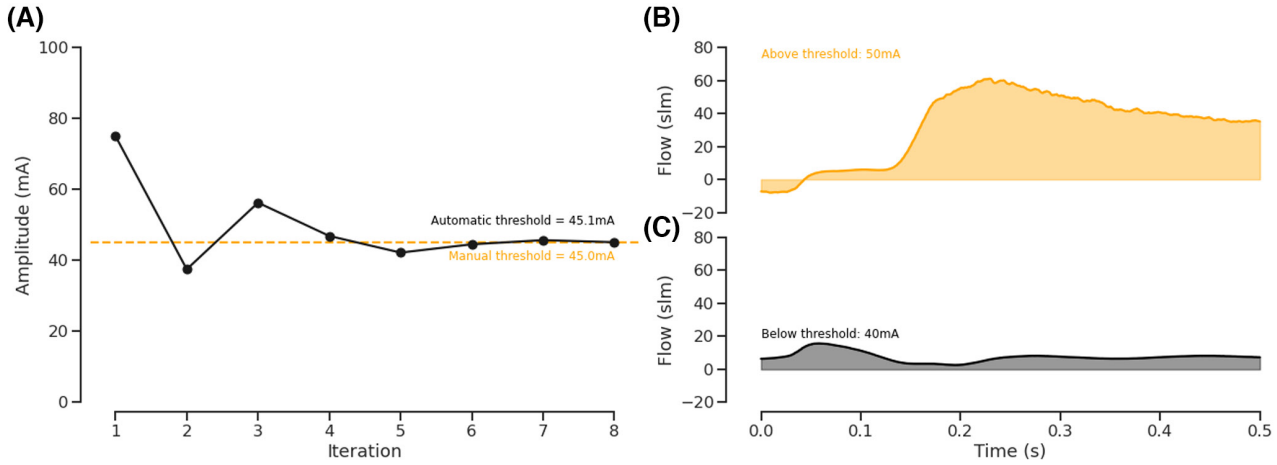

FIGURE 3 Automated threshold detection. (A) Detection of amplitude threshold using binary search. The stimulation amplitude is automatically varied, and the response measured. The amplitude is then adjusted based on the response to stimulation. This is repeated until the system converges on the threshold required for producing a respiratory response. Here, the closed-loop system converges on the manually measured threshold (shown in orange) in eight iterations, allowing rapid optimization of parameters. (B) Example respiratory response to a single pulse at 5 mA above the automatically detected threshold. There is a strong response to stimulation. (C) Example respiratory response to a single pulse at 5 mA below the automatically detected threshold. There is no response to stimulation. slm, standard liters per minute. [Color figure can be viewed at wileyonlinelibrary.com]

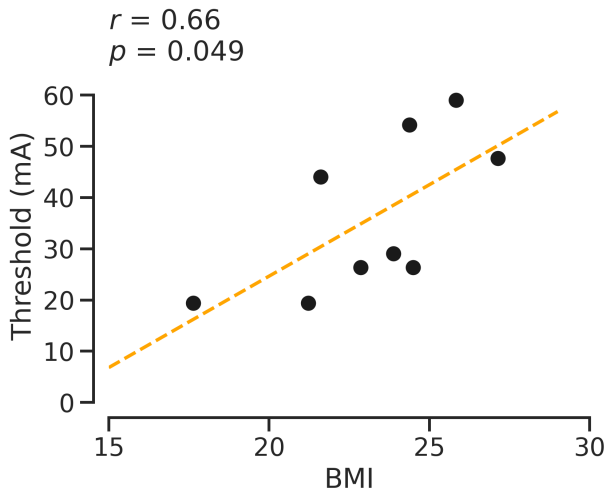

FIGURE 4 Correlation between amplitude threshold and participant BMI. The individually optimized amplitude required to produce a response is moderately correlated with the participant's BMI (Pearson's $r = 0.66$, $p = 0.049$). Points represent individual participants; the orange dashed line shows the line of best fit. BMI, body mass index. [Color figure can be viewed at wileyonlinelibrary.com]

between maximum and minimum measured thresholds measured over three trials) of 2.15 ± 1.61 mA. Repeating measurements of thresholds within a single subject to better characterize the level of intra-individual variation in threshold measurements showed a mean threshold across trials of 25.43 ± 0.70 mA (range 24.02–26.37 mA), confirming a low level of intra-individual variation in threshold measurements.

3.4 | Pulse train delivery

Application of pulse trains using bilateral stimulation with the optimized parameters produces a strong respiratory response. Stimulation with 200 ms pulse trains at 50 Hz with biphasic, charge balanced square waves with a pulse width of 100 µs per phase and an amplitude of 125% of the automatically determined threshold reliably produces a diaphragm contraction with an average volume inhaled of 457.03 ± 97.89 mL (range 398.27–725.16 mL).

An example of the respiratory response to an optimized pulse train is shown in Figure 5. The stimulation electrode and parameters are automatically determined. A pulse train is then delivered synchronized with the respiratory cycle. In this example, a diaphragm contraction producing an inhaled volume of 463 mL is produced by stimulation during quiet breathing. This demonstrates that it is possible to produce meaningful diaphragm contractions synchronized with respiration using automatically determined parameters.

Repeating these measurements with unilateral stimulation produces a mean inhaled volume with right-sided unilateral stimulation of 235.57 ± 24.20 mL (range 206.49–286.23 mL) and to left-sided unilateral stimulation of 240.27 ± 69.56 mL (range 161.44–402.79 mL). There was no statistically significant difference in the inhaled volume produced by stimulation based on laterality ($p = 0.8591$, repeated-measures t-test). Bilateral stimulation produced a statistically significantly greater inhaled volume than both right-sided ($p < 0.0001$, repeated-measures t-test) and left-sided ($p = 0.0001$, repeated-measures t-test) unilateral

15251594, 2024, 3, Downloaded from https://onlinelibrary.wiley.com/doi/10.1111/aor.14593 by Test, Wiley Online Library on [19/05/2024]. See the Terms and Conditions (https://onlinelibrary.wiley.com/terms-and-conditions) on Wiley Online Library for rules of use; OA articles are governed by the applicable Creative Commons License

stimulation. Example responses to unilateral and bilateral stimulation using optimized parameters are shown in Figure 6, demonstrating a measurable diaphragm response to stimulation with unilateral stimulation and a larger induced inhaled volume with simultaneous bilateral stimulation with optimized parameters.

3.5 | Burst calibration

The automatically determined amplitude threshold using single pulses tends to overestimate the amplitude required to produce a reliable response using a 200 ms burst of stimulation at 50 Hz. Figure 7A shows the automated determination of the amplitude threshold using a full 10-pulse (200 ms) burst of stimulation rather than single stimulation pulses. In all cases, the threshold required for a reliable response to a 10-pulse burst was less than half of that required for a response to single pulses. This overestimation risks unnecessary power consumption, increasing the risk of off-target effects and producing discomfort in applications with conscious patients.

The automatically determined stimulation threshold for an example participant as a function of the length of the stimulation burst used for calibration is shown in Figure 7B. There is a significant difference between the threshold determined by single pulses and that required for activation with a 10-pulse burst. The use of doublet stimulation produces significantly more accurate estimates of the burst stimulation threshold, while triplet stimulation produces more accurate results again. The use of burst lengths greater than three pulses starts to produce diminishing returns, with little difference in the thresholds for three-pulse and five-pulse bursts.

This indicates that the use of short bursts allows for more accurate determination of individualized stimulation thresholds than the use of single pulses while still avoiding excessive power consumption and retaining efficiency.

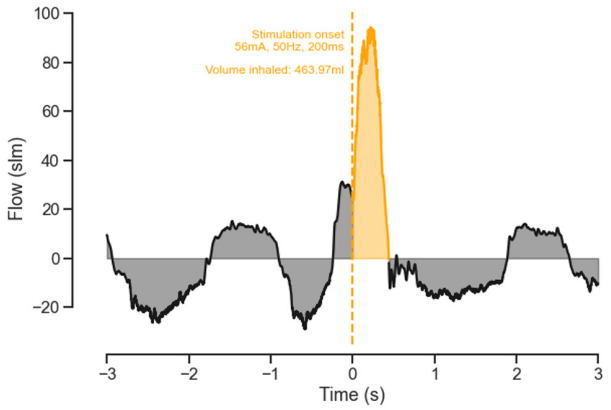

FIGURE 5 Pulse train delivery. A 200 ms pulse train at 50 Hz with an amplitude of 56 mA (125% of the automatically detected threshold) was delivered at the automatically chosen electrode. The response to stimulation is shown in orange. Pulse trains with automatically optimized parameters produce significant diaphragm activation with potential therapeutic applications. slm, standard liters per minute. [Color figure can be viewed at wileyonlinelibrary.com]

4 | DISCUSSION

Our results show that it is possible to implement a closed-loop system to automatically detect respiratory phase, deliver synchronized stimulation and adjust its parameters

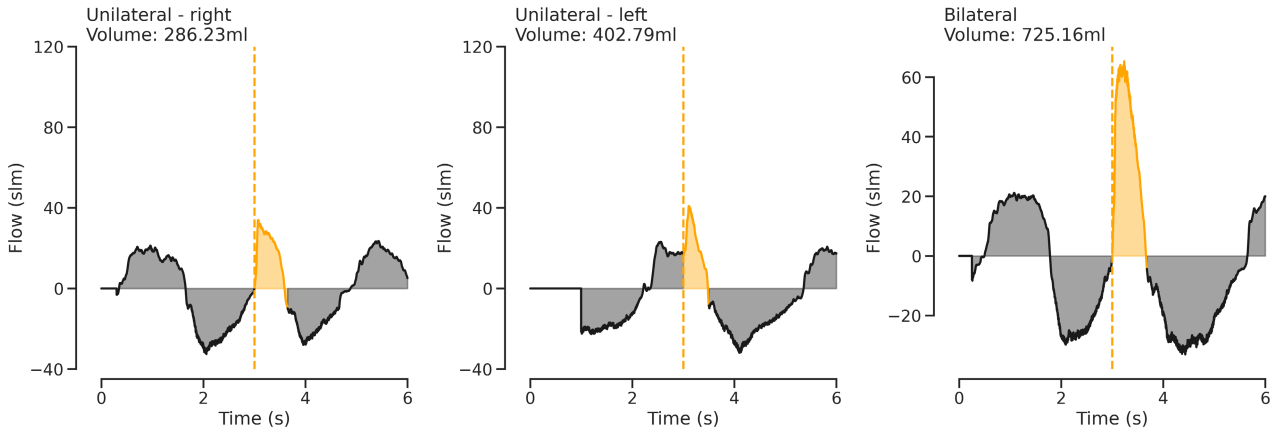

FIGURE 6 Effect of unilateral versus bilateral stimulation. The left and middle plots show response to stimulation with 200 ms pulse trains at 50 Hz with an amplitude of 125% of the automatically detected threshold using unilateral right- and left-sided stimulation. The right side shows the response to stimulation with both sides simultaneously. Bilateral stimulation with optimized parameters produces a significant diaphragm response, and this is significantly greater than the response to stimulation at either side unilaterally. slm, standard liters per minute. [Color figure can be viewed at wileyonlinelibrary.com]

15251594, 2024, 3, Downloaded from https://onlinelibrary.wiley.com/doi/10.1111/aor.14593 by Test, Wiley Online Library on [19/05/2024]. See the Terms and Conditions (https://onlinelibrary.wiley.com/terms-and-conditions) on Wiley Online Library for rules of use; OA articles are governed by the applicable Creative Commons License

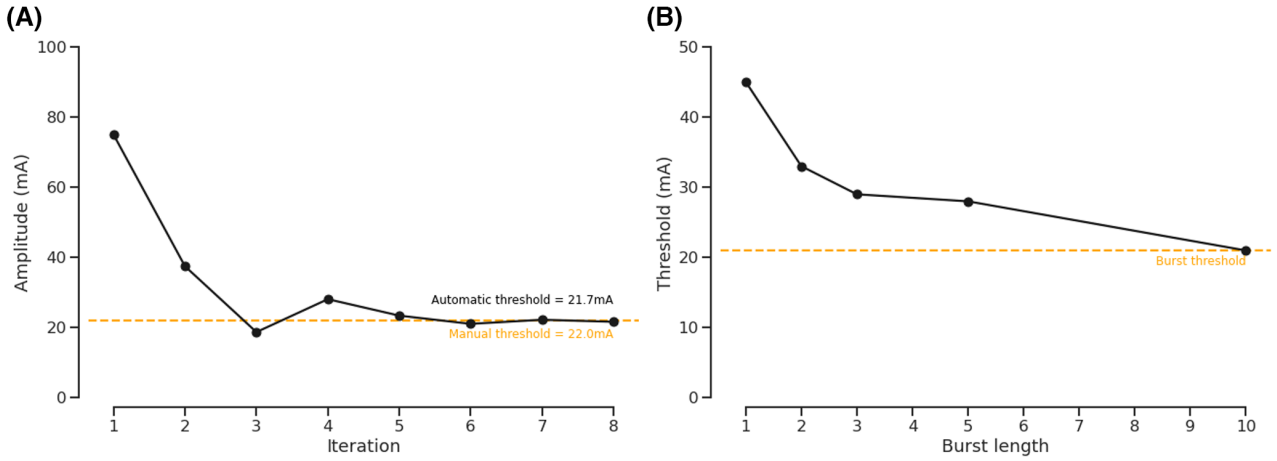

FIGURE 7 Effect of burst length on automated threshold detection. (A) Detection of amplitude threshold using binary search for a 10-pulse burst at 50 Hz (burst duration 200 ms). The automated system again converges on the manually determined threshold for producing a respiratory response. However, the threshold required for response to a burst is significantly lower than that required for a response to a single pulse. Individualizing stimulation amplitudes based on responses to single pulses may therefore overestimate the stimulation amplitude required. (B) Automatically determined threshold as a function of the length of bursts used for testing. The threshold required to produce a response to a single pulse is significantly higher than that for a 10-pulse burst. The use of doublets or triplets produces more accurate estimates, with diminishing returns with increasing burst durations. This allows efficient identification of burst thresholds using short bursts of stimulation. [Color figure can be viewed at wileyonlinelibrary.com]

based on the response to stimulation. This allows for stimulation to be reliably delivered during the inspiratory phase in the respiratory cycle, producing consistent results. This overcomes the problems with parameter sensitivity of non-invasive stimulation, making this a potential valuable treatment approach for mechanically ventilated patients.

We show that it is possible to deliver stimulation and automatically record the respiratory response. This system can then be used to automatically adjust stimulation parameters in order to maximize the diaphragm response produced. This overcomes the potential issues with electrode positioning and individual calibration, allowing an integrated, closed-loop system to be placed which will perform electrode selection and parameter adjustment itself. This is a significant step toward lowering the barriers to the clinical application of non-invasive phrenic nerve stimulation.

The feedback signal used, that is, respiratory flow, is recorded in line with a standard anesthetic circuit. This can therefore be integrated with existing ventilation systems without any adjustment, allowing straightforward application of this automated system to a clinical environment without additional specialized tools. The system then automatically synchronizes with the respiratory cycle, allowing it to be used with any ventilator settings without requiring any adjustments and minimizing the risk of producing asynchronies between the patient and the ventilator.

The system presented here is able to very rapidly determine individualized parameters, requiring only a few seconds to select the optimal electrode and determine the threshold required. This is beneficial for potential long-term application, where the system can continually update the required parameters in order to account for any changes in electrode position or stimulation parameters required over time. This ability to automatically track and maximize the diaphragm response has the potential to maintain meaningful contractions even when applied for prolonged periods.

This ability to automatically determine individualized parameters has significant advantages over comparable methods. Previous trials of external electrical stimulation have relied on detailed individual calibration of electrode position and parameters using diaphragm ultrasound and manual alteration of parameters until a response is observed,[17] requiring significant time commitment as well as specialist training. While methods such as trans-venous,[6] percutaneous,[8] and surgical[10] stimulation all require implantation procedures with the associated time and skilled staff required to carry out electrode placement and calibrate the response. We demonstrate that it possible to achieve individualized electrode position and parameter optimization rapidly and without the need for specialized skills using a closed-loop method to automatically adjust parameters. This potentially represents a method of achieving diaphragm activation which is not limited by the availability of trained specialists nor by the financial implications of significant specialist equipment limiting widespread application.

We further show that the use of short stimulation bursts such as doublets or triplets for individual calibration can

15251594, 2024, 3, Downloaded from https://onlinelibrary.wiley.com/doi/10.1111/aor.14593 by Test, Wiley Online Library on [19/05/2024]. See the Terms and Conditions (https://onlinelibrary.wiley.com/terms-and-conditions) on Wiley Online Library for rules of use; OA articles are governed by the applicable Creative Commons License

produce accurate estimates of the amplitude threshold for longer bursts as they improve the signal (respiratory flow driven by stimulated diaphragm contraction) to noise ratio over the use of single pulses. This provides advantages over the simpler single-pulse approach by avoiding overestimation of the required stimulation amplitude while still retaining energy efficiency and rapid iteration times. This results in reduced power consumption, which is a significant advantage for prolonged use, as well as reducing the likelihood of off-target effects such as contraction of overlying neck muscles. This has a further advantage in reducing the discomfort produced by activation of cutaneous afferent nerves, making non-invasive stimulation of the phrenic nerve feasible even in conscious patients.

It is important to note that the stimulation frequency of 50 Hz used here for non-invasive stimulation of the phrenic nerve is significantly greater than that typically used for implanted phrenic nerve stimulation using surgically implanted electrodes within the thorax[18] and is higher than the stimulation frequency used typically in these implanted settings based on animal models demonstrating fatigue at higher stimulation frequencies.[19] However, previous work on the response of the phrenic nerve to non-invasive stimulation suggests that higher frequencies are required to produce a reliable response non-invasively,[12] and this is within the range used in studies of non-invasive diaphragm pacing.[17] Furthermore, stimulation is delivered as short bursts intended to produce contractions for diaphragm exercise with significant rest periods between contractions rather than the regular pacing paradigm used in these studies, lessening the risk of a deleterious effect of stimulation with higher frequencies in this setting.

4.1 | Limitations

The system demonstrated here has been developed and tested on healthy volunteers. Detailed testing in an intensive care setting will be required in order to determine the long-term stability of these optimized parameters in this more challenging environment. Furthermore, while inhaled volume provides a useful proxy measure for diaphragm contraction in healthy participants, complementary measures of diaphragm function and inspiratory effect such as muscle ultrasound[20] or expiratory occlusion pressure[21] will need to be explored to assess this approach in the presence of parenchymal lung disease, where excessive diaphragm contraction could generate high dynamic transpulmonary driving pressure and injure the diaphragm itself.

Similarly, while it is possible to poll electrodes rapidly to detect a flow response during relaxed breathing in healthy individuals, allowing reliable detection of optimal electrodes even within a single respiratory cycle, this may not be possible in ventilated patients where the flow is dictated by the ventilator. In this context, it will likely be necessary to test the response at each electrode on sequential breaths, slightly extending the time required to reliably detect the optimal electrode.

Furthermore, it is important to note that the value of inducing diaphragm contractions to maintain diaphragm function is not necessarily applicable to all patients in intensive care units. Patients on assistive modes of ventilation where there is still some intrinsic diaphragm activity present driving respiration may benefit less from forced diaphragm contractions, while patients with significant pulmonary pathology may have further stress placed on their respiratory systems by forced contraction. Care must therefore be taken in translating these findings into the clinical setting.

5 | CONCLUSION

We demonstrate that the use of an automated system for individualization of stimulation parameters allows for reliable diaphragm activation using non-invasive stimulation with a simple application procedure and no need for manual calibration. This therefore represents a non-invasive system that can be easily applied using simple anatomical landmarks and no specialist skills which can robustly produce diaphragm contractions synchronized to normal respiration with individually optimized stimulation parameters.

These results represent a valuable steps toward an integrated system for closed-loop control of stimulation parameters for non-invasive phrenic nerve stimulation. This raises the possibility for simple, self-contained systems that can be applied in an intensive care setting to automatically maintain the diaphragm function of ventilated patients.

AUTHOR CONTRIBUTIONS

Conor Keogh, Francisco Saavedra, Sebastian Dubo, Pablo Aqueveque, Paulina Ortega, Jonathan Jarvis, Brian Andrews, and James J. FitzGerald conceived of and designed the studies. Adrian Poulton, Francisco Saavedra, Conor Keogh, Brian Andrews, Britam Gomez, Enrique Germany, Francisco Pastene, Daniela Pinto, and James J. FitzGerald designed and fabricated the equipment. Conor Keogh, Francisco Saavedra, Rodrigo Osorio, Brian Andrews, Sebastian Dubo, Britam Gomez, and James J. FitzGerald collected the data. Conor Keogh and Francisco Saavedra performed the analysis. Conor Keogh, Francisco Saavedra, Jonathan Jarvis, Brian Andrews, and James J. FitzGerald wrote the manuscript. Pablo Aqueveque, Jonathan Jarvis, Brian Andrews, and James J. FitzGerald supervised the project.

15251594, 2024, 3, Downloaded from https://onlinelibrary.wiley.com/doi/10.1111/aor.14593 by Test, Wiley Online Library on [19/05/2024]. See the Terms and Conditions (https://onlinelibrary.wiley.com/terms-and-conditions) on Wiley Online Library for rules of use; OA articles are governed by the applicable Creative Commons License

ACKNOWLEDGMENTS

The authors would like to thank the National Agency of Research and Development (ANID), Chile, FOVI220205 and the University of Oxford University Challenge Seed Fund for supporting this research. This work was further supported by the National Institute for Health Research (NIHR) through the NIHR Oxford Biomedical Research Centre and the UK Engineering and Physical Sciences Research Council (EPSRC) via the University of Oxford Clarendon Fund. Additionally, it was supported by Project FONDEQUIP EQM150114 and FONDECYT 1201543. The views expressed are those of the authors and not necessarily those of the funding bodies.

CONFLICT OF INTEREST STATEMENT

The authors declare no conflict of interest.

ORCID

Conor Keogh https://orcid.org/0000-0001-6549-5460

REFERENCES

1. Levine S, Nguyen T, Taylor N, Friscia ME, Budak MT, Rothenberg P, et al. Rapid disuse atrophy of diaphragm fibers in mechanically ventilated humans. New Engl J Med. 2008 Mar 27;358(13):1327–35.
2. Dres M, Goligher EC, Dubé BP, Morawiec E, Dangers L, Reuter D, et al. Diaphragm function and weaning from mechanical ventilation: an ultrasound and phrenic nerve stimulation clinical study. Ann Intensive Care. 2018;8(1):53.
3. Dow DE, Cederna PS, Hassett CA, Kostrominova TY, Faulkner JA, Dennis RG. Number of contractions to maintain mass and force of a denervated rat muscle. Muscle Nerve. 2004 Jul;30(1):77–86.
4. Onders RP. Functional electrical stimulation: restoration of respiratory function. Handb Clin Neurol. 2012;109:275–82.
5. Burgess LC, Venugopalan L, Badger J, Street T, Alon G, Jarvis JC, et al. Effect of neuromuscular electrical stimulation on the recovery of people with COVID-19 admitted to the intensive care unit: a narrative review. J Rehabil Med. 2021 Mar 1;53(3):jrm00164.
6. Dres M, On behalf of the RESCUE-2 Investigators Group. Temporary transvenous diaphragm neurostimulation in mechanically ventilated patients: per protocol results from the RESCUE-2 randomised controlled trial. Am J Respir Crit Care Med. American Thoracic Society International Conference Meetings Abstracts American Thoracic Society International Conference Meetings Abstracts. 2021 May;A4668.
7. Dres M, Gama de Abreu M, Merdji H, Müller-Redetzky H, Dellweg D, Randerath WJ, et al. Randomised clinical study of temporary transvenous phrenic nerve stimulation in difficult-to-wean patients. Am J Respir Crit Care Med. 2022 Feb 2;205:1169–78.
8. O'Rourke J, Soták M, Curley GF, Doolan A, Henlín T, Mullins G, et al. Initial assessment of the percutaneous electrical phrenic nerve stimulation system in patients on mechanical ventilation. Crit Care Med. 2020;48(5):e362.
9. Onders RP, Markowitz A, Ho VP, Hardacre J, Novitsky Y, Towe C, et al. Completed FDA feasibility trial of surgically placed temporary diaphragm pacing electrodes: a promising option to prevent and treat respiratory failure. Am J Surg. 2018 Mar 1;215(3):518–21.
10. Onders RP, Elmo MJ, Kaplan C, Katirji B, Schilz R. Extended use of diaphragm pacing in patients with unilateral or bilateral diaphragm dysfunction: a new therapeutic option. Surgery. 2014 Oct 1;156(4):776–86.
11. Kaufmann EM, Krause S, Geisshuesler L, Scheidegger O, Haeberlin A, Niederhauser T. Feasibility of transesophageal phrenic nerve stimulation. Biomed Eng Online. 2023 Jan 30;22(1):1–14.
12. Keogh C, Saavedra F, Dubo S, Aqueveque P, Ortega P, Gomez B, et al. Non-invasive phrenic nerve stimulation to avoid ventilator induced diaphragm dysfunction in critical care. Artif Organs. 2022;46:1988–97.
13. Severinghaus J. Electrophrenic respirator: description of a portable all-electronic apparatus. Anesthesiology. 1951 Jan 1;12(1):123–7.
14. Gandevia SC, McKenzie DK. Activation of the human diaphragm during maximal static efforts. J Physiol. 1985 Oct 1;367(1):45–56.
15. Shaw RK, Glenn WWL, Hogan JF, Phelps ML. Electrophysiological evaluation of phrenic nerve function in candidates for diaphragm pacing. J Neurosurg. 1980 Sep 1;53(3):345–54.
16. Mier A, Brophy C, Moxham J, Green M. Repetitive stimulation of phrenic nerves in myasthenia gravis. Thorax. 1992;47(8):640–4.
17. Bao Q, Chen L, Chen X, Li T, Xie C, Zou Z, et al. The effects of external diaphragmatic pacing on diaphragm function and weaning outcomes of critically ill patients with mechanical ventilation: a prospective randomized study. Ann Transl Med. 2022 Oct;10(20):1100.
18. Glenn WWL, Hogan JF, Loke JSO, Ciesielski TE, Phelps ML, Rowedder R. Ventilatory support by pacing of the conditioned diaphragm in quadriplegia. N Engl J Med. 1984;310(18):1150–5.
19. Oda T, Glenn WWL, Fukuda Y, Hogan JF, Gorfien J. Evaluation of electrical parameters for diaphragm pacing: an experimental study. J Surg Res [Internet]. 1981 Feb 1;30(2):142–53.
20. Haaksma ME, Smit JM, Boussuges A, Demoule A, Dres M, Ferrari G, et al. Expert consensus on diaphragm UltraSonography in the critically ill (EXODUS): a Delphi consensus statement on the measurement of diaphragm ultrasound-derived parameters in a critical care setting. Crit Care. 2022 Dec 1;26(1):99.
21. Bertoni M, Telias I, Urner M, Long M, Del Sorbo L, Fan E, et al. A novel non-invasive method to detect excessively high respiratory effort and dynamic transpulmonary driving pressure during mechanical ventilation. Crit Care. 2019 Nov 6;23(1):1–10.

How to cite this article: Keogh C, Saavedra F, Dubo S, Aqueveque P, Ortega P, Gomez B, et al. Closed-loop parameter optimization for patient-specific phrenic nerve stimulation. Artif. Organs. 2024;48:274–284. https://doi.org/10.1111/aor.14593

15251594, 2024, 3, Downloaded from https://onlinelibrary.wiley.com/doi/10.1111/aor.14593 by Test, Wiley Online Library on [19/05/2024]. See the Terms and Conditions (https://onlinelibrary.wiley.com/terms-and-conditions) on Wiley Online Library for rules of use; OA articles are governed by the applicable Creative Commons License